

Research Article

Griseofulvin/Carrier Blends: Application of Partial Least Squares (PLS) Regression Analysis for Estimating the Factors Affecting the Dissolution Efficiency

Annalisa Cutrignelli,¹ Adriana Trapani,¹ Angela Lopedota,¹ Massimo Franco,¹ Delia Mandracchia,¹ Nunzio Denora,¹ Valentino Laquintana,¹ and Giuseppe Trapani^{1,2}

Received 12 May 2011; accepted 28 July 2011; published online 9 August 2011

Abstract. The main aim of the present study was to estimate the carrier characteristics affecting the dissolution efficiency of Griseofulvin (Gris) containing blends (BLs) using partial least squares (PLS) regression analysis. These systems were prepared at three different drug/carrier weight ratios (1/5, 1/10, and 1/20) by the solvent evaporation method, a well-established method for preparing solid dispersions (SDs). The carriers used were structurally different including polymers, a polyol, acids, bases and sugars. The BLs were characterised at the solid-state by spectroscopic (Fourier transform infrared spectroscopy), thermoanalytical (differential scanning calorimetry) and X-ray diffraction studies and their dissolution behaviours were quantified in terms of dissolution efficiencies ($\log DE/DE_{\text{Gris}}$). The correlation between the selected descriptors, including parameters for size, lipophilicity, cohesive energy density, and hydrogen bonding capacity and $\log DE/DE_{\text{Gris}}$ (*i.e.*, DE and DE_{Gris} are the dissolution efficiencies of the BLs and the pure drug, respectively) was established by PLS regression analysis. Thus two models characterised by satisfactory coefficient of determination were derived. The generated equations point out that aqueous solubility, density, lipophilic/hydrophilic character, dispersive/polar forces and hydrogen bonding acceptor/donor ability of the carrier are important features for dissolution efficiency enhancement. Finally, it could be concluded that the correlations developed may be used to predict at a semiquantitative level the dissolution behaviour of BLs of other essentially neutral drugs possessing hydrogen bonding acceptor groups only.

KEY WORDS: blends/solid dispersions; dissolution efficiency; griseofulvin; PLS regression; prediction.

INTRODUCTION

The ever increasing interest in developing suitable dosage forms for the oral administration of drugs is due to the fact that it is the easiest and simplest route of administration allowing an improved compliance and quality of life of the patients. Unfortunately, most drugs both under development and even in clinical use are poorly water-soluble and consequently are endowed with a slow dissolution rate leading to a poor oral bioavailability. While for solubility enhancement, several approaches are known (1,2), the optimization of the dissolution rate of poorly water-soluble drugs requires improved technologies. To reach this goal represents one of the major challenges in drug delivery area. The solid dispersion (SD) technology is a well-established method for increasing dissolution rate and bioavailability of poorly water-soluble drugs (3–5). By this approach, a size reduction of drug particles in a hydrophilic or amphiphilic carrier occurs leading to a faster dissolution rate and

improved bioavailability. Solid dispersions (SDs) are generally prepared by two different methods, melting extrusion and solvent evaporation methods (6,7). Such processes generate both amorphous and crystalline SDs drug dispersions depending on the type of carrier used. Amorphous SDs occur when polymeric carriers (*e.g.*, polyvinylpyrrolidone, PVP) are employed while crystalline carriers including urea and sugars lead to crystalline SDs (6,7). In general, amorphous SDs dissolve faster compared to their crystalline alternatives, however they are not physically stable and during the shelf life may undergo unpredictable crystallisation (8).

To reduce development times and to obtain a more rational carrier selection, understanding of fundamental aspects of solid dispersion technique is essential. Several studies have pointed out the importance of both total- and partial-solubility parameters (δ_{tot} and δ_{d} , δ_{p} , δ_{h} , respectively) in determining dissolution properties and bioavailability of SDs (9,10). In line with these suggestions, Greenhalgh *et al.* (11) suggested that the total solubility parameters provide an indication of the miscibility/compatibility between drug and carrier in SD. It is noteworthy that, to date, rapid calculation of both partial and total solubility parameters for drugs and carriers can be made using computer softwares based on the group contribution procedures (12–14).

¹Dipartimento Farmaco-Chimico, Facoltà di Farmacia, Università degli Studi di Bari, Via Orabona 4, 70125 Bari, Italy.

²To whom correspondence should be addressed. (e-mail: trapani@farmchim.uniba.it)

Besides the solubility parameters, recent studies highlight also the importance for prediction purposes of further factors such as lipophilicity, melting point and hydrogen bonding drug/carrier interactions (7,8).

Using multivariate regression methods, we have recently derived quantitative structure–property relationships (QSPR) for predicting the dissolution rate enhancement of the model lipophilic drug oxazepam (Oxa) from blends (BLs) with 12 structurally different carriers at three different drug/carrier weight ratios (1/5, 1/10, and 1/20; 15). The BLs examined range from amorphous to partially and complete crystalline SDs [*i.e.*, SDs of first and second generation type according to the Vasconcelos *et al.* classification (8)], while systems such as Oxa/urea and Oxa/sorbitol BLs do not seem to form true solid dispersions at all. The computational models developed in the earlier study allow to estimate the dissolution efficiencies (16) of these BLs by using calculated carrier aqueous solubility, density, lipophilicity, the partial solubility parameters δ_a and δ_p , and an indicator variable accounting for the presence or absence of a sugar carrier.

The present study was aimed to estimate the factors affecting the dissolution efficiency of Griseofulvin (Gris) BLs by application of multivariate methods. Gris was chosen as another model drug, taking into account that it is an essentially neutral substance, like Oxa, but it is less lipophilic than Oxa and it does not possess hydrogen bonding donor groups (Table I). In this regard, several studies stressed the importance of hydrogen bonding formation between the dispersed drug and the carrier in the stabilisation of solid dispersions (7). It should be also noted that several studies on SDs of this antibiotic have previously been reported in literature (17–20) and in addition, a commercially available SD example of this drug is known [Gris-polyethylene glycol (PEG), 125 or 250 mg of active ingredient, Pedinol Pharmacal Inc (7)]. In particular, in these works, the following aspects

have been investigated: the factors influencing “solid solubility” and phase separation kinetics of Gris–PVP SD (17), the factors influencing the stability and dissolution properties of Gris–PVP SD (19) and the effect of hydrogen bonding properties on the maintenance of an amorphous state of Gris–CrosPVP SD (18).

MATERIALS AND METHODS

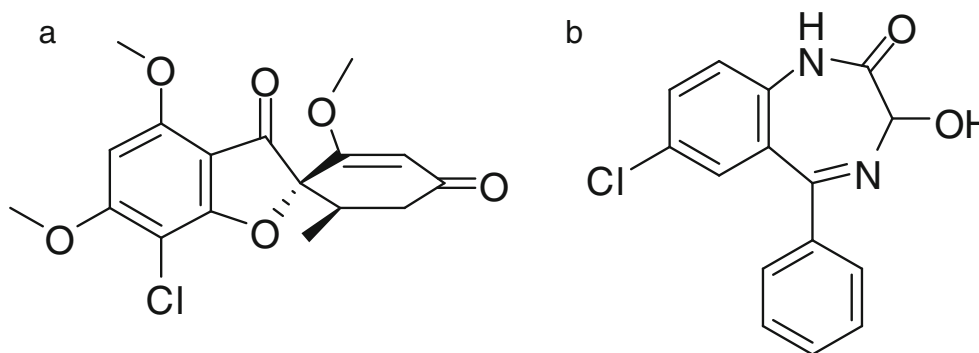
Chemicals

Gri, prednisolone, carbamazepine, polyethylene glycol 6000 (PEG 6000), PVP K-30, mannitol, citric acid, anhydrous lactose, urea, nicotinamide, succinic acid, sucrose, raffinose, and trehalose were purchased from Sigma-Aldrich (Milan, Italy). Etizolam was a gift of Farmades-Schering (Milan, Italy). Diazepam was extracted from capsules of Valium® 5 mg (Roche, Milan, Italy) purchased from a local drugstore as follows: 40 Valium® 5 mg capsules were opened and the resulting powder was treated with CHCl_3 (100 mL). The suspension was filtered through paper filter, dried (Na_2SO_4) and evaporated. Identity and purity of Diazepam was checked by gas chromatography and high-performance liquid chromatography (HPLC) traces. All reagents used for the preparation of the buffers were of analytical grade. Fresh deionized water was used in the preparation of the solutions. HPLC mobile phase was prepared from HPLC grade acetonitrile.

Chromatographic Analysis

HPLC analyses were carried out with a Waters Associates Model 590 pump equipped with a Waters 2487 UVVis 20 variable wavelength UV detector and a 20 μL loop injection valve. A reversed-phase symmetry C_{18} (15 cm \times 4.6 mm; 5 μm

Table I. Molecular Weight, Melting Point and Some Physicochemical Characteristics of Griseofulvin (a) and Oxazepam (b)



Compound	MW	MP (°C)	Sw (mg/l)	Log P	HBA groups ^a	HBD groups ^b
Griseofulvin	352.76	220	8.64	2	6	0
Oxazepam	286.71	206	179	2.8	3	2

Data from DrugBank (<http://www.drugbank.ca/drugs/DB00400>)

^a HBA, hydrogen bonding acceptor groups. ^b HBD, hydrogen bonding donor groups

particles) column in conjunction with a precolumn (Sentry Guard symmetry C18, 20×3.9 mm) was eluted with 45:55 (v:v) acetonitrile: 0.025 M phosphate buffer (pH 2.7) in isocratic mode. All analyses were performed in isocratic conditions. The flow rate of 1.0 mL/min was maintained, the column effluent was monitored continuously at 291 nm and the retention time of Gris was 7.5 min. The compounds were quantified by measuring the peak areas in relation to those of Gris standard solutions chromatographed under the same conditions. Calibration curves were prepared at 291 nm wavelength using methanol as solvent and they were linear ($r^2=0.999$) over the range of tested concentrations (1.4×10^{-3} to 2.7×10^{-6} M).

Preparation of Blends and Physical Mixtures of Gris/Carrier

Gris-loaded BLs were prepared by the solvent evaporation method with Gris and carrier (*i.e.*, PEG 6000, PVP K30, mannitol, citric acid, lactose, urea, nicotinamide, succinic acid, sucrose, raffinose, trehalose) at different weight ratios of 1:5, 1:10 or 1:20 and the resulting mixtures referred in the following as Gris/carrier 1/5, 1/10, 1/20 BL, respectively. In particular, the appropriate amount of Gris (75 mg) and carrier were thoroughly mixed in a mortar and then 50 mL of aqueous ethanol 80% (v/v) were added and the resulting mixture was gently heated at 37°C with a water bath. Next, the solvent was evaporated under reduced pressure (15 mmHg) at about 40°C and the residue, dried under vacuum for 3 h, was stored for at least overnight in a desiccator. Prior further use, the sample was pulverised using a mortar and pestle and the powder was passed through a 250 µm (mesh n. 60) sieve.

The physical mixtures (PMs) were prepared at the same weight ratio by thoroughly mixing in a mortar the drug and carrier. The resulting mixtures were passed through a 250 µm (mesh n. 60) sieve and denoted as PM 1/5, 1/10 and 1/20, respectively. The preparation of each BL or PM was performed at least in triplicate.

Fourier Transform Infrared Spectroscopy

Fourier transform-infrared spectroscopy (FTIR) spectra of pure drug and BLs were obtained on a Perkin-Elmer 1600 FTIR spectrometer using KBr discs (2 mg sample in 200 mg KBr). The scanning range was 450–4,000 cm^{-1} and the resolution was 1 cm^{-1} . Eight scans were performed for each IR spectrum and calibration of the instrument was repeated periodically.

Thermal Analysis

Differential scanning calorimetry (DSC) thermograms were obtained by a Mettler Toledo DSC 822e Star[®] 202 System (Mettler Toledo, Switzerland) equipped with an automatic thermal analysis programme. About 5 mg of each sample were placed in an aluminium pan (40 µL capacity and 0.1 mm thickness) press-sealed with a perforated aluminium cover of 0.1 mm thickness. An empty pan of the same type was used as reference. DSC measurements were performed by heating the sample from 25°C up to 300°C at a rate of 5°C/min under a dry nitrogen flow of 50 cm^3/min . Indium (purity

99.99%) was used to calibrate the temperature and heat flow. Reproducibility was checked by running the sample in triplicate.

X-ray Analysis

Powder X-ray diffraction (PXRD) patterns were recorded on a Philips PW 1830 powder X-ray diffractometer using Cu K α radiation, a voltage of 30 kV and a current of 55 mA. Patterns were obtained using a scanning range between 4° and 35° in 2 θ with 20s/°. Three scans were performed for each PXRD spectrum.

Dissolution Studies

Dissolution experiments were carried out in triplicate using freshly prepared samples. These experiments were conducted using a VK 8000 dissolution paddles test apparatus (Vankel, USP Apparatus 2) at 37°C and a rotation speed of 60 rpm. Each sample (equivalent to 15 mg of Gris) was added to the dissolution medium consisting of 900 mL of 0.05 M potassium phosphate buffer pH 7.4. At predetermined time intervals, 2 mL of the medium were withdrawn and filtered through a 0.22 µm membrane filter (Millipore®, cellulose acetate, Milan, Italy) in thermostated test tubes. The initial volume of dissolution was maintained by adding 2 mL of dissolution medium. About 1 mL of the clear filtrate was analysed by HPLC using an injection volume of 20 µL. The dissolution experiments were followed up to 24 h and the results are means of three determinations with relative standard deviation (CV) values <5%.

Dissolution Efficiency

The BL dissolution profiles were analysed using the dissolution efficiency (DE) parameter (16), defined as the area under the dissolution curve up to a certain time t , expressed as a percentage of the area of the rectangle arising from 100% dissolution in the same time. DE values were calculated by the following equation:

$$DE = y \, dt / 100 \, t$$

where, y is the drug percent dissolved at time t . In this work, all dissolution efficiencies were calculated with t equal to 1,440 min.

The areas under the curve were calculated using the GraphPad Prism (v. 3 for Windows) software (GraphPad Software, San Diego, CA, USA). The BL dissolution properties were quantified as $\log DE/DE_{\text{Gris}}$, where DE and DE_{Gris} are the dissolution efficiencies of the BLs and the pure drug (*i.e.*, the intrinsic DE of the drug), respectively.

Selection of Carriers and Models Development

In the present study, we considered the following 11 carriers: the polymers PEG 6000 and PVP K-30, the polyol mannitol, the acids citric and succinic, the bases urea and nicotinamide and, finally, the sugars anhydrous lactose, sucrose, raffinose and trehalose. All these carriers have been already used in the SD technology. To derive the Models able

to predict $\log DE/DE_{\text{Gris}}$ the steps followed were: (1) preparation of the BLs and determination of the corresponding $\log DE/DE_{\text{Gris}}$ values, (2) selection of 18 potentially relevant and computed carrier descriptors, (3) selection of pertinent descriptors through principal component analysis (PCA) combined with a cluster analysis based on correlation coefficients among variables, (4) use of the partial least squares (PLS) projection to latent structures method to find the relationship between the experimentally determined $\log DE/DE_{\text{Gris}}$ values and the computed pertinent descriptors.

Molecular Descriptors Selection

The molecular descriptors of the carriers used in this study [e.g., molecular weight (MW), molecular volume (MV), melting point (MP), log of octanol/water partition coefficient (C log P), molecular refractivity (MR), total number of hydrogen bonds (Htot), number of oxygen and nitrogen atoms (nON), number of OH and NH groups (nOHNH), topological polar surface area (TPSA), water solubility (log Sw), total and partial solubility parameters δ_{tot} and δ_{d} , δ_{p} , δ_{h} , respectively, density, superficial tension, and the two indicator variables of a polymeric (*Ipol*) and a sugar carrier (*I sug*)] were calculated as previously reported (15) and are listed in Table II.

Regression Analysis

PCA and the PLS methods were performed using both the Unscrambler (v. 7.5, CAMO ASA, Oslo, Norway) and Statgraphics. Centurion XV (StatPoint, Inc.; www.statgraphics.com) software. Cluster analysis was carried out using StatGraphics Centurion XV software.

RESULTS

Solid-State Characterization

To estimate possible interactions between drug and carrier in the solid state, the carbonyl stretching region (1,550–1,750 cm^{-1}) in the FTIR spectra of the freshly

prepared BLs was examined. Figure 1 shows the FTIR spectra of selected BLs along with that of the pure drug. The FTIR spectrum of Gris showed two strong absorption bands at 1,707 and 1,659 cm^{-1} , due to phenyl- and cyclohexenyl-ketone C=O, respectively (Fig. 1). In the FTIR spectra of PEG 6000-, lactose-, trehalose-, sucrose-, raffinose-, and mannitol-based BLs, the absorption bands at 1,707 and 1,659 cm^{-1} , were present even though at reduced intensities. It is indicative of the absence of hydrogen bond interactions between the drug and these carriers. The absorption bands at 1,707 and 1,659 cm^{-1} are absent in the FTIR spectra of PVP-, urea-, nicotinamide-, citric acid-, and succinic acid-based BLs. In these spectra, only a broad band characteristic of the pure carrier was generally detected in the 1,550–1,750 cm^{-1} wavelengths range that likely masks the drug absorption bands and in these cases no conclusion could be drawn about drug-carrier interactions. FTIR spectra of the PMs displayed essentially the same characteristics observed for the corresponding BLs (data not shown).

DSC and PXRD analyses were performed to gain insight on the amorphous/crystalline state of BLs examined. DSC profiles of Gris and selected BLs are shown in Fig. 2. The DSC thermogram of pure Gris powder showed a single endothermic peak at 220°C, corresponding to the melting of the drug. Such a peak was not observed in the DSC curves of some BLs. Thus, PEG-based systems exhibited a melting endotherm at about 62°C attributable to the melting of the polymer, while no trace of the endothermic peak at 220°C occurs. Similarly, no endothermic peaks at 220°C were detected in the case of citric acid-, urea-, succinic acid-, nicotinamide-based BLs where only peaks attributable to the melting of the carrier were observed. In the case of mannitol and trehalose containing BLs, the endothermic peak corresponding to the melting of the drug occurs even though at lower temperature (217°C) and with reduced intensity. The peak of Gris at 220°C in sucrose-, lactose- and raffinose-based BLs presumably is masked by endothermic peaks at about 220°C that are present in the DSC profile of the pure carriers. Furthermore, PVP-based BLs were characterised by DSC curves indicative of an amorphous physical state with Tg of about 163°C (Fig. 2).

Table II. The Molecular Descriptors of the Carriers used in this Study^a

Carrier	MW	MV	MP	MR	C log P	TPSA	Htot	nON	nOHNH	δ_{tot}	δ_{d}	δ_{p}	δ_{h}	Log Sw	Sup tens	density	Ipol	I sug pos
PEG 6000	1,031	906.3	62	25.19	0.05	243.6	50	24	2	21.54	17.88	2.96	11.63	5.05	40.4	1.117	1	0
PVP K30	794	628.4	165	21.71	-0.82	142.16	21	14	0	24.26	21.41	5.79	9.83	-2.35	65.7	1.307	1	0
Mannitol	182.17	114.1	166	3.88	-2.05	121.37	18	6	6	39.84	19.03	10.28	33.46	0.98	99.8	1.596	0	0
Citric acid	192.13	109	153	3.68	-1.56	132.13	18	7	4	31.38	20.92	8.24	21.89	6.76	103.9	1.762	0	0
Lactose	342.3	193.6	200	7.07	-4.4	189.53	30	11	8	43.96	24.19	11.23	34.94	-0.36	116.4	1.8	0	1
Urea	60.06	49.5	133	1.41	-1.66	69.12	8	3	4	35.55	19.43	21.62	20.47	1.4	55.3	1.212	0	0
Nicotinamide	122.13	101.3	131	3.35	-0.21	55.99	6	3	2	27.23	19.96	13.11	13.08	-0.56	54.8	1.204	0	0
Succinic acid	118.1	83.8	188	2.41	-0.53	74.6	10	4	2	24.3	17.94	6.66	14.97	5.37	61.6	1.408	0	0
Sucrose	342.3	192.8	185	7.07	-3.09	189.53	30	11	8	44.35	24.68	11.32	35.07	-0.42	113	1.77	0	1
Raffinose	504.44	277.8	118.5	10.44	-4.66	268.68	43	16	11	41.35	23.19	8.79	33.09	-1.76	120.7	1.81	0	1
Trehalose	342.3	193.6	98	7.07	-3.26	189.53	30	11	8	43.96	24.19	11.23	34.94	-0.45	110.8	1.76	0	1

MW molecular weight, MV molecular volume, MP melting point, MR molecular refractivity, C log P log of octanol/water partition coefficient, TPSA topological polar surface area, Htot total number of hydrogen bonds, nON number of oxygen and nitrogen atoms, nOHNH number of OH and NH groups, log Sw water solubility

^aMelting point (MP) values were obtained from the following sources: The Merck Index., 14th ed. MJ O'Neil ed. Whitehouse Station, NJ; 2006. Chemfinder website (www.chemfinder.com). The Analytical Profile of Drug Substances and Excipients. Brittain HG ed. San Diego: Academic Press; 1994

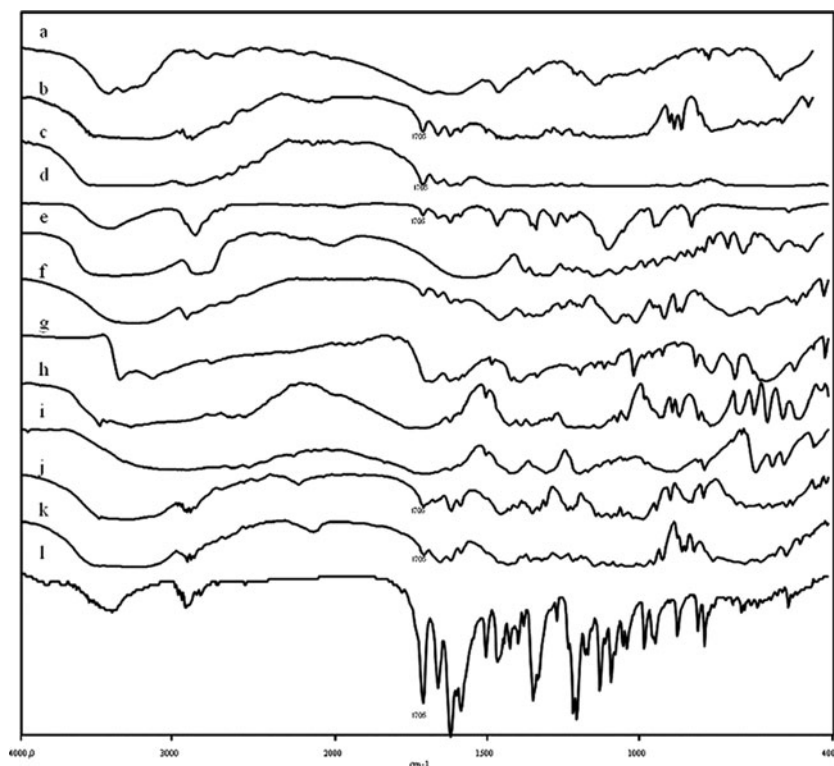


Fig. 1. FTIR spectra of pure drug and 1/10 Gris/carriers BLs: *a* Gris/urea, *b* Gris/lactose, *c* Gris/sucrose, *d* Gris/PEG 6000, *e* Gris/PVP K30, *f* Gris/mannitol, *g* Gris/nicotinamide, *h* Gris/citric acid, *i* Gris/succinic acid, *j* Gris/trehalose, *k* Gris/raffinose, *l* pure Gris. For a sake of concision, only FTIR spectra of 1/10 Gris/carriers BLs are shown. The corresponding spectra of 1/5 and 1/20 Gris/carriers BLs are available on request

Altogether, these findings suggest that a decrease in crystallinity of Gris occur consequent to BL formation. It was further supported by the analysis of X-ray diffraction spectra. Thus, the X-ray diffraction spectra of the Gris/carrier 1/10 systems displayed diffraction peaks corresponding to the characteristic reflections of crystalline Gris at 2θ 10.8°, 13.3°, 14.7° and 16.6°. These last reflections were chosen as distinctive for the estimation of BL amorphous/crystalline character since they are favourably positioned and intense enough. The distinctive diffraction peaks were markedly attenuated in PEG-, citric acid-, urea-, succinic acid-, nicotinamide- and lactose-based BLs. In the case of PVP-, mannitol-, trehalose-, sucrose- and raffinose containing BLs, no distinctive peaks were detected. The behaviour of 1/5 and 1/20 systems was similar to that observed for the above described 1/10 weight ratio BLs (Fig. 3).

Dissolution Studies

Figure 4a–c shows the dissolution profiles of all BLs examined and the corresponding DE values are reported in Table III. As can be seen from the reported data, pure Gris dissolution showed a DE value of 40.45 while in the cases of trehalose- and raffinose-based BLs high DE values (up to 94.83 and 81.05, respectively) were observed. PEG containing BLs showed DE values lower than pure Gris (*i.e.*, 32.88 and 38.13 for 1/5 and 1/10 BLs, respectively) and only a little improvement for the 1/20 system (*i.e.*, 45.71). Similarly, a little increase in DE values were observed for lactose- and urea-based BLs indicating

that these carriers as PEG 6000 are, on the whole, detrimental for DE enhancement. Similar trends can be pointed out considering the time enabling the 50% dissolution of the active ingredient (*i.e.*, $t_{50\%}$) for both pure drug and BLs (data not shown). Thus, pure Gris, PEG-, urea-, lactose-based BLs displayed $t_{50\%}$ values ≥ 24 h. In contrast, trehalose- and raffinose-containing BLs as well as some PVP-containing systems showed $t_{50\%}$ values of 10–20 min. Sucrose, mannitol, succinic and citric acid and nicotinamide BLs were characterised by a variable $t_{50\%}$ in the range of 1 h (*i.e.*, sucrose and mannitol) and 3 h (*i.e.*, succinic and citric acid and nicotinamide). Definitely, based on the $t_{50\%}$ values, the dissolution rate kinetic can be considered fast for trehalose-, raffinose- and some PVP-containing systems, intermediate for mannitol-, succinic- and citric acid and nicotinamide BLs, slow for the pure drug and PEG-, urea-, lactose-based systems. In Fig. 4d, for a sake of concision, the dissolution profiles of selected PMs were also reported and compared with the corresponding BLs. As shown, marked differences in DEs were observed; being the DEs of BLs greater than the corresponding PMs. In particular, the DE enhancement ratios (defined as the ratio between the DE of BL and that of the corresponding PM) calculated for the systems trehalose 1/10, trehalose 1/20, raffinose 1/10 and raffinose 1/20 are 1.96, 2.19, 2.12 and 2.27 respectively.

Models Development

Among the 18 descriptors devised for the carriers, the selection of pertinent predictors was made as previously

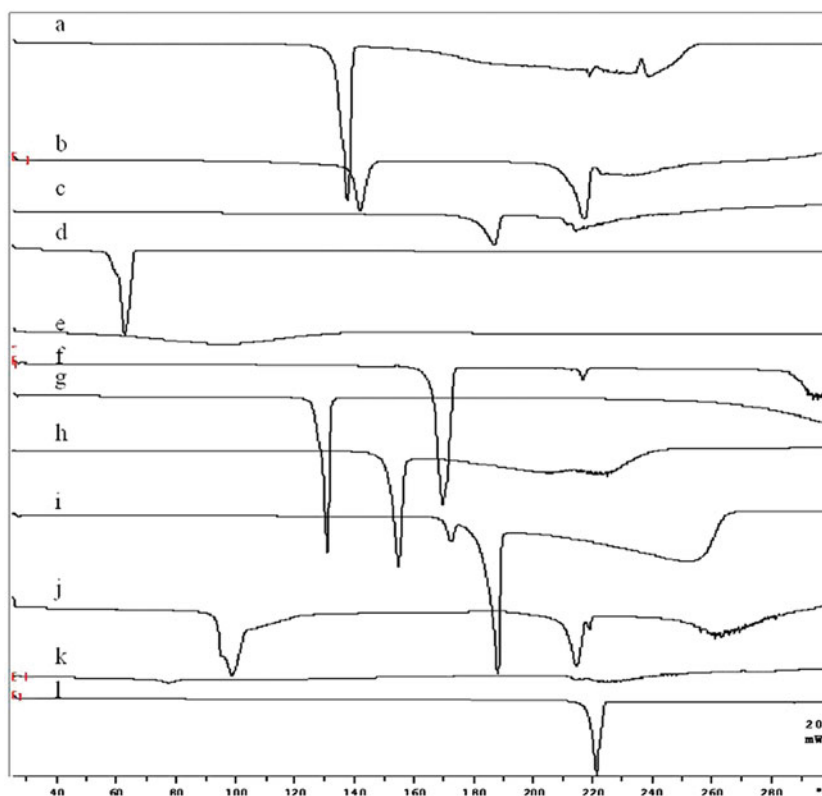


Fig. 2. DSC curves of pure drug and 1/10 Gris/carriers BLs. For legend, see Fig. 1. For a sake of concision, only DSC curves of 1/10 Gris/carriers BLs are reported. The corresponding DSC curves of 1/5 and 1/20 Gris/carriers BLs and pure carriers are available on request

reported using PCA and cluster analysis (15). Thus, the nine calculated predictors MW, C log P, log Sw, density, δ_{tot} , δ_{d} , δ_{p} , TPSA and nON, together with both the experimental MP and the two indicator variables *Ipol* and *Isug*, were selected and used in the regression analysis. Since at least five compounds per variable are needed for deriving a reliable model, we considered only models containing no more than six descriptors being 33 the Gris BLs prepared. Moreover, taking into account that the PLS method is particularly suited for the extraction of a few highly significant factors from large sets of correlated descriptors, in this study, correlation between the selected descriptors and log DE/DE_{Gris} values were established by this regression method. The best PLS model on five principal components yielded a six-parameter equation which explains more than 60% of the log DE/DE_{Gris} data variance (model 1, Table IV). Figure 5 shows the relationship between observed *vs.* predicted log DE/DE_{Gris} by model 1.

We considered also PLS models with a number of descriptors lower than 6 using nOHNH instead of nON as predictor of hydrogen bonding capacity. While nON is predictor of hydrogen bonding acceptor capacity, nOHNH takes into account mainly of hydrogen bonding donor interactions. In this context, it was found that the best PLS model was model 2 in Table IV. As it can be seen in Table IV, this model is characterised by a five-parameter equation which explains more than 60% of the log DE/DE_{Gris} data variance and utilises the nOHNH as descriptor instead of δ_{p} and *Isug*.

A careful examination of the models derived indicates that those with six and five descriptors are comparable from a statistical point of view both in terms of coefficient of determination (R^2) and predictive ability (Q^2).

DISCUSSION

The main objective of this work was to estimate the factors affecting the dissolution efficiency of Gris containing BLs by application of multivariate methods. For this purpose, BLs with 11 structurally different carriers at three different drug/carrier weight ratios (1/5, 1/10 and 1/20) were prepared by the solvent evaporation method.

Solid-state characterization studies indicate that the examined BLs range from amorphous (*e.g.*, PVP) to semi-crystalline (*e.g.*, PEG) and to crystalline (*e.g.*, mannitol and trehalose) systems. However, it should be taken into account that the degree of crystallinity for the Gris/carrier systems cannot be quantified with higher accuracy since detection limits of 5% crystallinity or lower have been reported when amorphous/crystalline mixtures are analysed by powder X-ray diffractometry (21). The disappearance of a melting peak in the DSC profile in general indicates that the drug is present in amorphous state or that it is dissolved in the solid state (22). It can be invoked for PEG-, citric acid-, urea-, succinic acid-, nicotinamide-based BLs. From the obtained data, it can be concluded that most of the BLs examined from a physicochemical point of view can be classified as “solid solutions” SDs according to Janssens and Van den Mooter

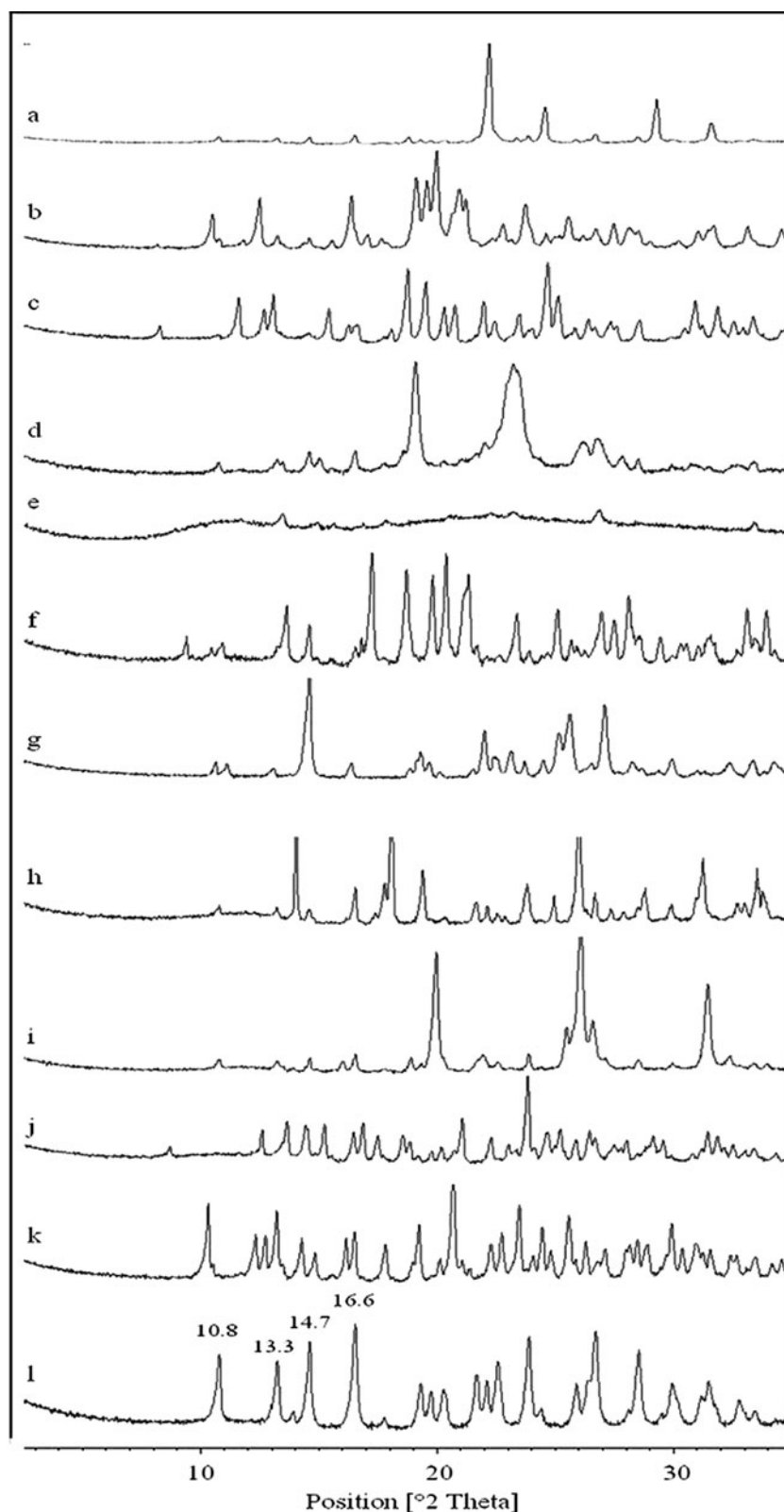


Fig. 3. XRD of spectra of pure drug and 1/10 Griseofulvin/carriers BLs. For legend, see Fig. 1. For a sake of concision, only XRD of spectra of 1/10 Griseofulvin/carriers BLs are shown. The corresponding XRD of spectra of pure carriers are available on request

classification (7) since most of the carriers examined are crystalline in nature. In contrast, PVP-based BLs should be classified as “glass solutions” since these systems consist of an

amorphous carrier. In the case of “glass solutions”, the drug can be either molecularly dispersed or form an amorphous precipitate into its carrier (7). It is interesting to note that

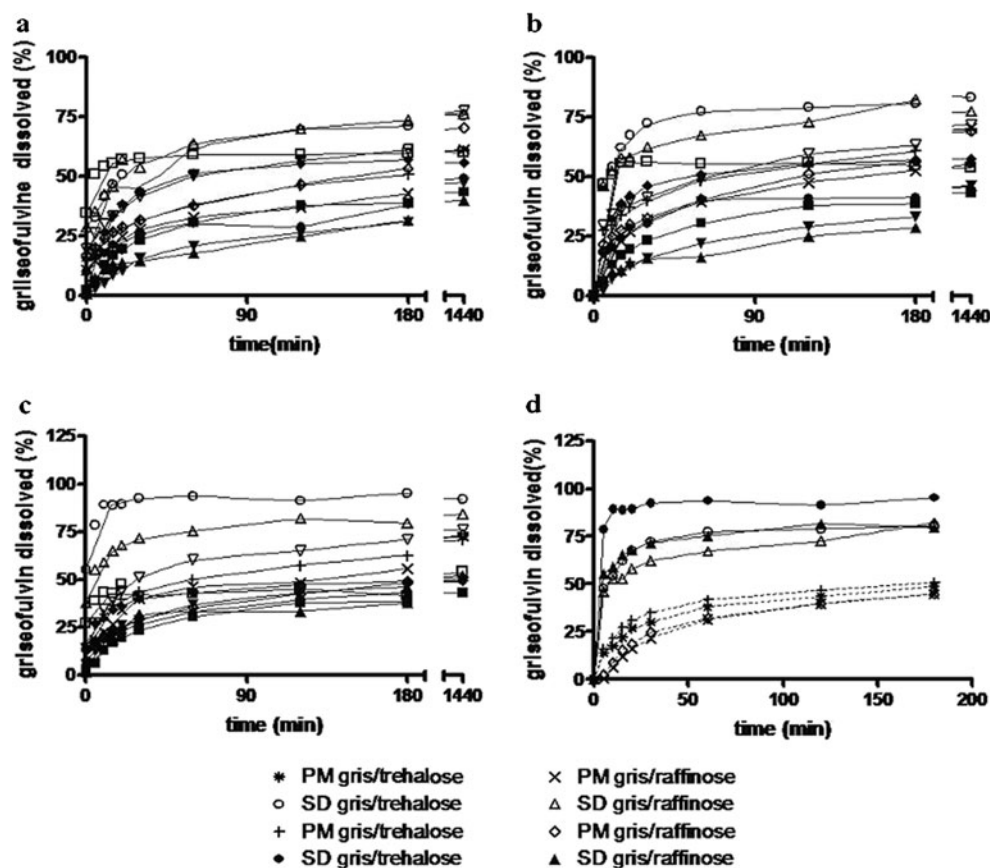


Fig. 4. Dissolution profiles in 0.05 M potassium phosphate buffer pH 7.4 at 37°C ($n=3$) of the BLs examined and selected PMs: **a** 1/5 BLs, **b** 1/10 BLs, **c** 1/20 BLs. *Black square* pure Gris, *filled triangle* Gris/PEG 6000, *filled down-pointing triangle* Gris/urea, *filled diamond* Gris/sucrose, *filled circle* Gris/lactose, *white square* Gris/PVP K30, *empty triangle* Gris/raffinose, *empty down-pointing triangle* Gris/mannitol, *empty diamond* Gris/nicotinamide, *empty circle* Gris/trehalose, *multiplication symbol* Gris/succinic acid, *plus sign* Gris/citric acid; **d** selected PMs

among the carriers that favour the formation of glass solutions besides PVP, there are also sugars as trehalose and sucrose (7). Overall, taking into account the preparative method of BLs and their solid-state and dissolution features, most of these systems can be considered SDs with variable DE ranging from detrimental to efficient and most efficient DE as a consequence of the different nature of the carriers investigated. From a statistical point of view, the observed data set is appropriate to derive a relationship relating DE and carrier characteristics.

The Gris dissolution efficiency was more than doubled in the case of trehalose 1/10 BLs, 1/20 BLs and raffinose 1/20 BLs but the observed detrimental effect played by PEG at 1/5 and 1/10 weight ratios was somewhat surprising taking into account that a commercially available Gris-PEG SD is known (7). It can be hypothesised that in the case of trehalose or raffinose glass solutions occur together with an improved drug wettability. A decrease in crystallinity of the drug together with an improved drug wettability are considered important factors in determining the enhanced drug dissolution rate from SDs (23). However, it should be noted that further mechanisms have been proposed to account for the increase in dissolution rate of drugs from their SDs (5,24–26).

Evaluation of the Models

As for the PLS analyses, it is important to outline briefly the physicochemical significance of the models derived for predicting the enhancement in dissolution rate of the lipophilic drug Gris from BLs. Model 1 is characterised by the same six independent variables (carrier descriptors) previously found for Oxa BLs (15). The unique difference is represented by the positive correlation between $\log DE/DE_{\text{Gris}}$ and density indicating that the higher the carrier density, the higher the dissolution rate of the dispersion. The significance of the remaining independent variables should be as previously reported and namely, the negative correlation between $\log DE/DE_{\text{Gris}}$ and $\log S_w$ indicates that the higher the carrier aqueous solubility, the lower the dissolution rate of the dispersion. This result may be interpreted assuming that the rate of release is controlled by that of the carrier [*i.e.*, the so-called carrier-controlled model (5)]. Under these conditions, if the water-soluble carrier dissolution is faster than drug, it can limit further dissolution of drug particles from BL/SDs. On the basis of the aforementioned carrier-controlled model, also the role of $C \log P$ can be reasonably interpreted. In fact, taking into account that lipophilicity is negatively correlated with aqueous solubility (27) it follows that enhancement in carrier lipophilicity influences positively

Table III. Dissolution Efficiencies [Means of at Least Three Determinations, Standard Deviation (CV) <5%] of the BLs Examined

BLs	DE	DE/DEGris	Log DE/DEGris observed	Log DE/DEGris predicted mod. 1	Log DE/DEGris predicted mod. 2
Gris	40.45	1	0		
Gris/PEG 6000 1/5	32.88	0.813	-0.0899	-0.0164	0.01460
Gris/PVP 1/5	60.26	1.49	0.173	0.137	0.121
Gris/mannitol 1/5	68.73	1.70	0.230	0.272	0.294
Gris/citric acid 1/5	56.70	1.40	0.147	0.168	0.173
Gris/lactose 1/5	42.95	1.06	0.0260	0.124	0.102
Gris/urea 1/5	40.04	0.990	-0.00442	0.00447	0.00281
Gris/nicotinamide 1/5	61.52	1.52	0.182	0.161	0.158
Gris/succinic acid 1/5	52.80	1.31	0.116	0.170	0.134
Gris/sucrose 1/5	55.31	1.37	0.136	0.221	0.217
Gris/raffinose 1/5	55.31	1.83	0.261	0.191	0.228
Gris/trehalose 1/5	73.96	1.83	0.262	0.219	0.207
Gris/PEG 6000 1/10	38.13	0.943	-0.0256	-0.0164	0.01460
Gris/PVP 1/10	53.09	1.31	0.118	0.137	0.121
Gris/mannitol 1/10	66.93	1.66	0.218	0.272	0.294
Gris/citric acid 1/10	64.91	1.61	0.205	0.168	0.173
Gris/lactose 1/10	47.51	1.17	0.0699	0.124	0.102
Gris/urea 1/10	38.89	0.961	-0.0171	0.00447	0.00281
Gris/nicotinamide 1/10	62.56	1.55	0.189	0.161	0.158
Gris/succinic acid 1/10	62.46	1.54	0.189	0.170	0.134
Gris/sucrose 1/10	55.25	1.37	0.135	0.221	0.217
Gris/raffinose 1/10	74.30	1.84	0.264	0.191	0.228
Gris/trehalose 1/10	82.94	2.05	0.312	0.219	0.207
Gris/PEG 6000 1/20	45.61	1.13	0.0521	-0.0164	0.01460
Gris/PVP 1/20	47.57	1.18	0.0704	0.137	0.121
Gris/mannitol 1/20	72.84	1.80	0.255	0.272	0.294
Gris/citric acid 1/20	67.28	1.66	0.221	0.168	0.173
Gris/lactose 1/20	47.20	1.17	0.0670	0.124	0.102
Gris/urea 1/20	46.74	1.16	0.0628	0.00447	0.00281
Gris/nicotinamide 1/20	60.77	1.50	0.177	0.161	0.158
Gris/succinic acid 1/20	65.22	1.61	0.207	0.170	0.134
Gris/sucrose 1/20	48.2	1.19	0.0761	0.221	0.217
Gris/raffinose 1/20	81.05	2.00	0.302	0.191	0.228
Gris/trehalose 1/20	94.83	2.34	0.370	0.219	0.207

the drug dissolution rate. The negative correlation of the partial solubility parameter δ_d and the positive one of δ_p indicated that the carrier should possess an appropriate

balance between non-polar (dispersive) and polar interactions for improving the dissolution rate of BLs/SDs. From model 1 emerges another important point and namely the

Table IV. Predictive Power of the Devised PLS Models

Descriptors and statistical evaluation	Model 1 regression coefficients	Model 1 standardised regression coefficients	Model 2 regression coefficients	Model 2 standardised regression coefficients
Log Sw	-0.0341	-0.943	-0.0315	-0.870
Density	0.853	2.10	0.678	1.68
δ_d	-0.0503	-1.15	-0.0303	-0.694
<i>I</i> <i>sub</i> <i>g</i>	0.148	0.666		
C log P	0.111	1.63	0.114	1.66
δ_p	0.00441	0.190		
nNHOH			0.0250	0.768
Intercept	0.0847	0.00	-0.0977	0.00
Samples	33		33	
R^{2a}	0.617		0.630	
Q^{2b}	0.417		0.472	
N_{PC}^c	5		5	
PRESS ^d	0.219		0.198	

^a R^2 is the coefficient of determination

^b Q^2 (an assessment of the 'internal' predictive ability of the model), is the cross validated coefficient of determination

^c N_{PC} is the number of principal components

^d PRESS is the prediction error of sum of squares

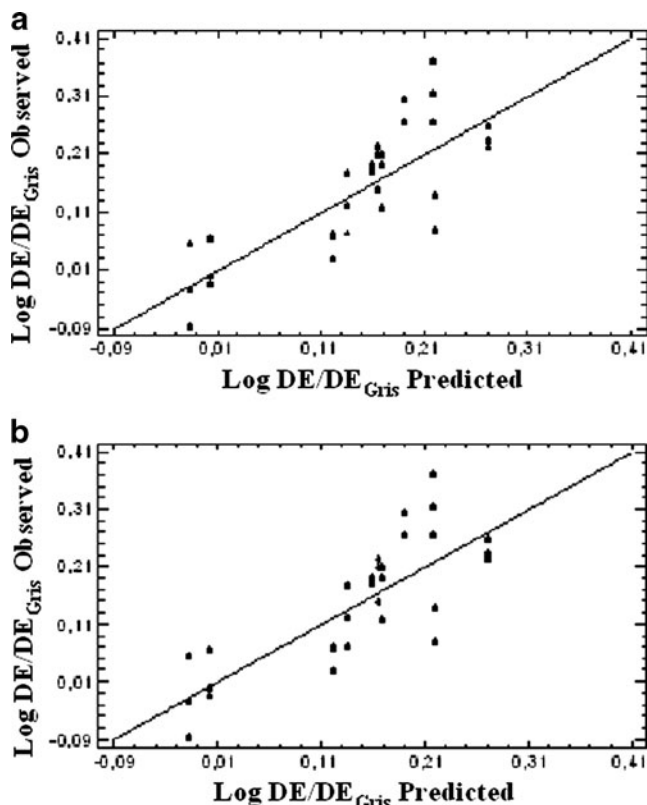


Fig. 5. Observed vs. predicted Log DE/DE_{Gris} according to **a** model 1 and **b** model 2

positive value associated to the coefficient of *Isug* suggesting that sugar carriers are favourable for improving the dissolution rate. To account for the discrepancy observed about the correlation with the density (positive in the case of Gris and negative for Oxa) it should be taken into account that high carrier density can bring about drug segregation in the BL. On the other hand, high carrier density can negatively affect the porosity of the mixture. Therefore, the effects of carrier density can be opposite as for dissolution properties of the BL and the resulting outcome can change also depending on the drug physicochemical properties. As mentioned, besides the water solubility, a considerable difference between the two drugs

considered is that Oxa can establish both hydrogen bonding acceptor and donor interactions with the carrier, while Gris can only form hydrogen bonding acceptor ones (Table I).

The good DE values of the Gris/raffinose 1/20, and Gris/trehalose 1/20 BLs should be also related to the fact that in these glass solutions the drug loading is at lowest level (*i.e.*, 5% *w/w*) and it is well known that, in general, decreasing the drug loading, the dispersion dissolution efficiency greatly improves.

The relative importance of each descriptor to the model 1 was evaluated by ranking the magnitudes of the standardised coefficients (Table IV). They are obtained by transforming the set of values of each descriptor to possess a mean of 0 and a variance of 1 (28). Ranking the standardised coefficients shows that density (*i.e.*, standardised coefficient 2.10) is the most important descriptor in model followed by C log P (standardised coefficient 1.63) and so on (Table IV). It is interesting to note that ranking the standardised coefficients previously found for Oxa BLs (15) it results that *Isug* (*i.e.*, standardised coefficient 0.815) is the most important descriptor in the model derived followed in the order by density, log Sw, C log P, δ_p and δ_d with standardised coefficients -0.723 , -0.322 , 0.0809 , 0.0806 and -0.0104 , respectively. Hence, it should be pointed out that even though model 1 is characterised by the same six independent variables previously found for Oxa BLs, the relative importance of each descriptor is different. In the case of Gris BLs, the carrier density is most important while for Oxa BLs the sugar nature of the carrier is the main descriptor.

Another interesting result of the PLS analyses is that, in the case of Gris BLs, also the model 2 work well and from a statistical point of view is comparable with model 1. The main difference is that model 2 utilises the nOHNH as descriptor instead of δ_p and *Isug*. The positive correlation of nOHNH with log DE/DE_{Gris} indicates that the higher the hydrogen bonding donor capacity of the carrier, the higher the dissolution rate of the dispersion. From model 2, the relevance of the carrier hydrogen bonding donor capacity for improving dissolution efficiency is pointed out and it has already been suggested from a qualitative point of view in several reports (7,17). On the other hand, it may be assumed that the significance of the descriptors δ_p and *Isug* in model 1 in some extent, is equivalent to hydrogen bonding donor capacity of the carrier. In fact, besides δ_p accounting for polar effects, a sugar carrier is characterised by a number of $-OH$ groups which are involved in hydrogen bonding donor interactions.

Table V. Predictive Power of the Devised PLS Models

Drug	N° HBA or HBD groups ^a	Carrier	Log DE/DE _{drug} observed	Log DE/DE _{drug} predicted
Prednisolone	5 (HBA) 3 (HBD)	Trehalose	0.00945	0.795 ^b
Prednisolone	5 (HBA) 3 (HBD)	Raffinose	0.0863	0.780 ^b
Carbamazepine	1 (HBA) 1 (HBD)	Trehalose	0.117	0.795 ^b
Carbamazepine	1 (HBA) 1 (HBD)	Raffinose	0.173	0.780 ^b
Diazepam	2 (HBA)	Trehalose	0.164	0.219 ^c /0.207 ^d
Diazepam	2 (HBA)	Raffinose	0.252	0.191 ^c /0.228 ^d
Etizolam	3 (HBA)	Trehalose	0.196	0.219 ^c /0.207 ^d
Etizolam	3 (HBA)	Raffinose	0.267	0.191 ^c /0.228 ^d

^a N° of HB acceptor (HBA) or donor (HBD) groups

^b Predicted value according to model 1 derived for Oxa BLs (15)

^c Predicted value according to model 1 derived for Gris BLs

^d Predicted value according to model 2 derived for Gris BLs

Application of the Models Developed

Whatever validated QSPR model can be expected to reliably predict the property examined only for samples falling within the training set while, for samples outside the training set, the predicted values could be less reliable, as they are extrapolations. In this study, the training set was assembled using 33 DE values for Gris BLs prepared from 11 structurally different carriers at three different drug/carrier weight ratios (1/5, 1/10 and 1/20). These DE values were determined by us and this warrants that the technique and equipment used to obtain the DE values were exactly the same. Therefore, the models developed in this study, like for those previously reported for Oxa BLs, besides the estimation of the factors affecting the dissolution efficiency of these systems, can be rigorously applied to predict the DE of BLs with drug/carrier weight ratios ranging between 1/5 and 1/20 because they are strictly representative of the training set used. However, we wished all the same to test the predictive power of Oxa/BLs and Gris/BLs correlations for the dissolution behaviour of BLs of other essentially neutral drugs and hence outside the training set. Thus, we attempted to predict the DE values for a testing set of four compounds constituted by prednisolone, carbamazepine and diazepam, etizolam possessing hydrogen bonding donor/acceptor and hydrogen bonding acceptor groups, respectively (Table V). The experimental $\log DE/DE_{\text{drug}}$ values of the BLs constituted by these drugs with trehalose or raffinose (drug/carrier weight ratios 1/20) were determined and compared with the values predicted by the Oxa/BLs and Gris/BLs correlations. As shown in Table V, drugs with hydrogen bonding donor/acceptor properties (*i.e.*, prednisolone and carbamazepine) are markedly overestimated by the Oxa/BLs model, while the Gris/BL correlations yielded values close enough to the observed ones in the case of diazepam and etizolam. In these last cases, the $\log DE/DE_{\text{drug}}$ values with trehalose were slightly overestimated by the Gris/BLs models, while using raffinose these models slightly underestimated the $\log DE/DE_{\text{drug}}$ values. Likely, these deviations occur since these compounds are not represented in the training set. In conclusion, it seems that the models derived may be used to predict at a semiquantitative level the dissolution behaviour of BLs of other essentially neutral drugs possessing hydrogen bonding acceptor groups only.

CONCLUSIONS

The computational models developed in this study can be used to quantify the $\log DE/DE_{\text{Gris}}$ using calculated carrier descriptors. Model 1 herein derived points out that, for dissolution efficiency enhancement, important features of the carrier are its aqueous solubility, its lipophilic/hydrophilic character and a good compromise between dispersive and polar forces. The importance of the density of the carrier is related to its effects on porosity of the dispersion and drug segregation in the mixture. The importance of hydrogen bonding acceptor/donor carrier ability is pointed out in models 2 that may be considered very similar to model 1. However, the relative importance of each descriptor is different. Thus, in the case of Gris BLs the carrier density is the most

important factor, while for Oxa BLs the sugar nature of the carrier is the main descriptor. These models work quite well allowing us to obtain quantified results and providing deeper insight into the factors governing the dissolution efficiency of this BL/SDs. On the other hand, the similarity of the models herein derived with those previously found for Oxa BLs leads us to conclude that the factors affecting the dissolution rate of essentially neutral substances are those above mentioned. Finally, it seems that the correlations developed may be used to predict at a semiquantitative level the dissolution behaviour of BLs of other essentially neutral drugs possessing hydrogen bonding acceptor groups only.

Future work should be devoted to estimate the factors affecting the dissolution efficiency of BLs containing lipophilic drugs being acid or base in nature.

ACKNOWLEDGMENTS

We thank Dr. Jörg Breitreutz (Westphalien Wilhelms University, Münster, Germany) for having provided us the SPWin, v. 2.1 software.

Conflict of interest None

REFERENCES

1. Strickley RG. Solubilizing excipients in oral and injectable formulations. *Pharm Res.* 2004;21:201–30.
2. Trapani A, Laquintana V, Lopodota A, Franco M, Latrofa A, Talani G, *et al.* Evaluation of new propofol aqueous solutions for intravenous anesthesia. *Int J Pharm.* 2004;278:91–8.
3. Serajuddin ATM. SD of poorly water-soluble drugs: early promises, subsequent problems, and recent breakthroughs. *J Pharm Sci.* 1999;88:1058–66.
4. Leuner C, Dressmann J. Improving drug solubility for oral delivery using SDs. *Eur J Pharm Biopharm.* 2000;50:47–60.
5. Craig DQM. The mechanisms of drug release from solid dispersions in water-soluble polymers. *Int J Pharm.* 2002;231:131–44.
6. Vasconcelos T, Sarmiento B, Costa P. Solid dispersions as strategy to improve oral bioavailability of poor water soluble drugs. *Drug Discov Today.* 2007;12:1068–75.
7. Janssens S, Van den Mooter G. Review: physical chemistry of solid dispersions. *J Pharm Pharmacol.* 2009;61:1571–86.
8. Vipagunta SR, Wang Z, Hornung S, Krill SR. Factors affecting the formation of eutectic solid dispersions and their dissolution behaviour. *J Pharm Sci.* 2007;96:294–304.
9. Hancock BC, York P, Rowe RC. The use of solubility parameters in pharmaceutical dosage form design. *Int J Pharm.* 1997;148:1–21.
10. Barra J, Bustamante P, Doelker E. Use of the solubility parameter and surface energy concepts in the formulation of solid dosage forms. *STP Pharma Sci.* 1999;9:293–305.
11. Greenhalgh DJ, Williams AC, Timmins P, York P. Solubility parameters as predictors of miscibility in SDs. *J Pharm Sci.* 1999;88:1182–90.
12. Fedors RF. A method for estimating both the solubility parameters and molar volumes of liquids. *Polym Eng Sci.* 1974;14:147–54.
13. Hansen CM. Hansen solubility parameters—a user's handbook. Boca Raton: CRC; 2000.
14. Breitreutz J. Prediction of intestinal drug absorption properties by three-dimensional solubility parameters. *Pharm Res.* 1998;15:1370–5.
15. Cutrignelli A, Lopodota A, Trapani A, Boghetich G, Franco M, Denora N, *et al.* Relationship between dissolution efficiency of

- oxazepam/carrier blends and drug and carrier molecular descriptors using multivariate regression analysis. *Int J Pharm.* 2008;358:60–8.
16. Khan CA, Rhodes CT. The concept of dissolution efficiency. *J Pharm Pharmacol.* 1975;27:48–9.
 17. Vasanthavada M, Tong W-Q, Joshi Y, Kislalioglu MS. Phase behaviour of amorphous molecular dispersions II: role of hydrogen bonding in solid solubility and phase separation kinetics. *Pharm Res.* 2005;22:440–8.
 18. Shibata Y, Fujii M, Kokudai M, Noda S, Okada H, Kondoh M, *et al.* Effect of characteristics of compounds on maintenance of an amorphous state in solid dispersion with crospovidone. *J Pharm Sci.* 2007;96:1537–47.
 19. Al-Obaidi H, Brocchini S, Buckton G. Anomalous properties of spray dried solid dispersions. *J Pharm Sci.* 2009;98:4724–37.
 20. Greenhalgh DJ, Cook W. Relationship between drug and carrier solubility parameters and dissolution of SD systems. *J Pharm Pharmacol.* 2000;52(Supplement):299.
 21. Rumondor ACF, Taylor LS. Application of partial least squares (PLS) modelling in quantifying drug crystallinity in amorphous solid dispersions. *Int J Pharm.* 2010;398:153–60.
 22. Tran PH-L, Tran TT-D, Lee KH, Kim D-J, Lee B-J. Dissolution-modulating mechanism of pH modifiers in solid dispersion containing weakly acidic or basic drugs with poor water solubility. *Expert Opin Drug Deliv.* 2010;7:647–61.
 23. Van den Mooter G, Wuyts M, Bleton N, Busson R, Grobet P, Augustijns P, *et al.* Physical stabilisation of amorphous ketocanazole in SDs with polyvinylpyrrolidone K25. *Eur J Pharm Biopharm.* 2001;12:261–9.
 24. Dubois JL, Ford JL. Similarities in the release rates of different drugs from polyethylene glycol 6000 dispersions. *J Pharm Pharmacol.* 1985;37:494–5.
 25. Craig DQM, Newton JM. The dissolution of nortriptyline HCl from polyethylene glycol solid dispersions. *Int J Pharm.* 1992;78:175–82.
 26. Sjökvist-Saers E, Craig DQM. An investigation into the mechanisms of dissolution of alkyl *p*-aminobenzoates from polyethylene glycol solid dispersions. *Int J Pharm.* 1992;83:211–9.
 27. Yalkowsky SH, Valvani SC. Solubility and partitioning I: solubility of nonelectrolytes in water. *J Pharm Sci.* 1980;69:912–22.
 28. Chari R, Qureshi F, Moschera J, Tarantino R, Kalonia D. Development of improved empirical models for estimating the binding constant of a β -cyclodextrin inclusion complex. *Pharm Res.* 2009;26:161–71.